Ultra-high Sensitivity Wavefront Sensing for Extreme-AO

Olivier Guyon

Subaru Telescope, NAOJ, 650 N. A'ohoku Pl., Hilo, HI, 96720, USA

ABSTRACT

A new wavefront sensing scheme derived from curvature wavefront sensing is presented. Non-linear Curvature wavefront sensing (NLCWFS) is a scheme derived from conventional curvature wavefront sensing. NLCWFS uses four defocused pupil images and a non-linear wavefront reconstruction. NLCWFS is largely achromatic and does not require a flat (<1 rad RMS) wavefront to operate: it is therefore very robust, and is an attractive alternative to less efficient Shack-Hartmann wavefront sensing. For low order aberrations, sensitivity gains corresponding to 5 and 8 stellar magnitudes can be achieved over the conventional Shack-Hartmann sensor on respectively a 8-m telescope and a 30-m telescope.

Keywords: Adaptive Optics, Coronagraphy

1. INTRODUCTION

The most common types of wavefront sensor (WFS) used in current AO systems, Shack-Hartmann and curvature, both have poor sensitivity to low order aberrations, especially if the WFS is designed for "high order" wavefront reconstruction.[1] This effect, also referred to as "noise propagation", limits the performance of AO systems unless the guide star is very bright. Noise propagation will push the AO system to be optimized either for bright stars (maximize the number of corrected mode at the expense of loosing sensitivity on the low order modes, which dominate the turbulence) or faint stars (optimize signal-to-noise ratio on the measurement of low order aberrations by restricting the number of modes corrected).

Direct imaging of exoplanet from ground-based telescopes requires WFS techniques which can simultaneously offer a high degree of correction and a very high sensitivity to low order aberrations. The goal of this paper is to offer such a solution by modification of the curvature WFS technique.

It is shown in §2, the most common types of wavefront sensors (Shack-Hartman and curvature) make a relatively inefficient use of incoming photons, especially for low order aberrations (this is known as the "noise propagation" problem). This limitation can be solved by using non-linear information in the curvature wavefront sensor frames (§3). Performance of this "non-linear Curvature Wavefront Sensor" scheme is quantified and discussed in §4.

2. SENSITIVITY TO LOW ORDER ABERRATIONS IN EXISTING WAVEFRONT SENSORS

2.1. SHACK-HARTMANN SENSORS

In a Shack-Hartmann (SH) WFS, the wavefront slope is measured for each subaperture as a motion of the corresponding focal plane spot. The low sensitivity of the SH WFS is due to the angular size of these spots, which is at best λ/r_0, and can be even larger if the subaperture size is smaller than r_0: this spot size is considerably larger than the diffraction limit of the telescope. For example, estimation of Tip-Tilt in a SH WFS is obtained by measuring the average of the spot centroids over all subapertures. For a total number of photons N in the WFS, the measurement error is therefore $\alpha/\sqrt{N}$ in the photon noise limit, where α is the spot size. Ideally, it should be possible to measure Tip-Tilt with a $\lambda/(D\sqrt{N})$ accuracy, taking advantage of the full angular resolution of the telescope. The difference in flux sensitivity, $(\alpha/(\lambda/D))^2$, is considerable in a visible WFS on a 8-m telescope where $\lambda/D = 15$mas, $\alpha = 0.6$arcsec and $(\alpha/(\lambda/D))^2 = 1500$. Measuring Tip-Tilt with a SH WFS

Further author information: (Send correspondence to Olivier Guyon.)
Olivier Guyon.: E-mail: guyon@naoj.org, Telephone: 1 808 934 5901

requires, for the same level of accuracy, 1500 times more photons than should ideally be necessary. This analysis can be generalized to other modes than Tip-Tilt, and the loss in sensitivity due to noise propagation decreases as the spatial frequency increases. The SH WFS is nearly optimal for sensing aberrations with spatial frequencies similar to the subaperture sampling in the pupil, but is very inefficient for low order aberrations. An equivalent representation of the noise propagation effect is to consider that a sine wave wavefront aberration is best sensed by combining (interfering) light from points of the pupil separated by about half the period of the wavefront aberration. The SH WFS, unfortunately, prevents such combinations from happening by optically isolating light from a subaperture from light from other subapertures.

As the number of subapertures is increased around and beyond $(D/r_0)^2$ in a SH WFS, the spot sizes increase due to diffraction by subapertures, and SH WFS sensitivity to low order aberrations further degrades. Reaching very high levels of correction is therefore constrained by the need for many subapertures on one side, and the loss of sensitivity for low order aberrations on the other side.

2.2. CURVATURE SENSORS

Curvature WFS suffer from the same "noise propagation". In a curvature WFS, wavefront curvature is measured as a contrast between inside and outside pupil images, and a linear relationship exists between the two quantities.[2] The range of defocus over which this linear relationship exists is however limited:

- As shown in Figure 1, on the left, a phase aberration at a given spatial frequency will propagate away from the pupil plane into a curvature signal, with a strength which grows as the defocus distance increases. Beyond some propagation distance, Fresnel propagation will however cancel this intensity signal (turning it back to phase, which cannot be detected - this is the "Talbot effect"). The intensity signal periodically oscillates with defocus distance, and the linear relationship between wavefront curvature and constrast between the two defocused pupil images is only limited to the first "half-period" of this oscillation (about 1500 km in the example given in Figure 1).
- As shown in Figure 1, on the right, low order aberrations like tip-tilt distort the defocused pupil images and the simple subtraction between the two images fails to recover the phase curvature: the two images "don't line up" anymore. For tip-tilt, this is a pure offset between the two images, but the distortion becomes more complicated for other aberrations.

The linear range imposed by both effect decreases as the wavefront aberration's spatial frequency increases: in higher order curvature systems, the defocused images have to be pushed closer to the pupil plane to maintain linearity. Figure 1, on the left, shows that phase is converted into intensity signal at an optimal distance from the pupil (slightly less than 1000 km in the example given in the figure). This optimal distance is a function of spatial frequency and grows larger for low order aberrations. As the defocused pupil images are acquired closer to the pupil plane to maintain linearity, the sensitivity to low order aberrations becomes poorer.

2.3. MITIGATION OF NOISE PROPAGATION IN A CURVATURE WAVEFRONT SENSOR

In a SH WFS, noise propagation is due to the optical chopping of the pupil: the loss in sensitivity cannot be recovered after the lenslet array.

In the Curvature WFS however, the loss in sensitivity is not due to the optical design, but is introduced by the requirement that the signal (contrast) should be linear with wavefront phase curvature. Mitigation of noise propagation effects occurs at two levels:

- Pupil distortions (Figure 1, right) become smaller in closed loop: the curvature WFS, unlike the SH WFS, can benefit from the wavefront correction.
- Since this linearity exists over a wider range of defocus distance for low spatial frequencies, it is possible to measure low spatial frequencies at larger defocus distance and low spatial frequencies at smaller defocus distance. This scheme, described in detail in Guyon et al. (2008), can mitigate noise propagation in a curvature WFS, and simulations have shown that a 1.5 magnitude gain in sensitivity is recovered on a 188-elements system on a 8-m telescope.

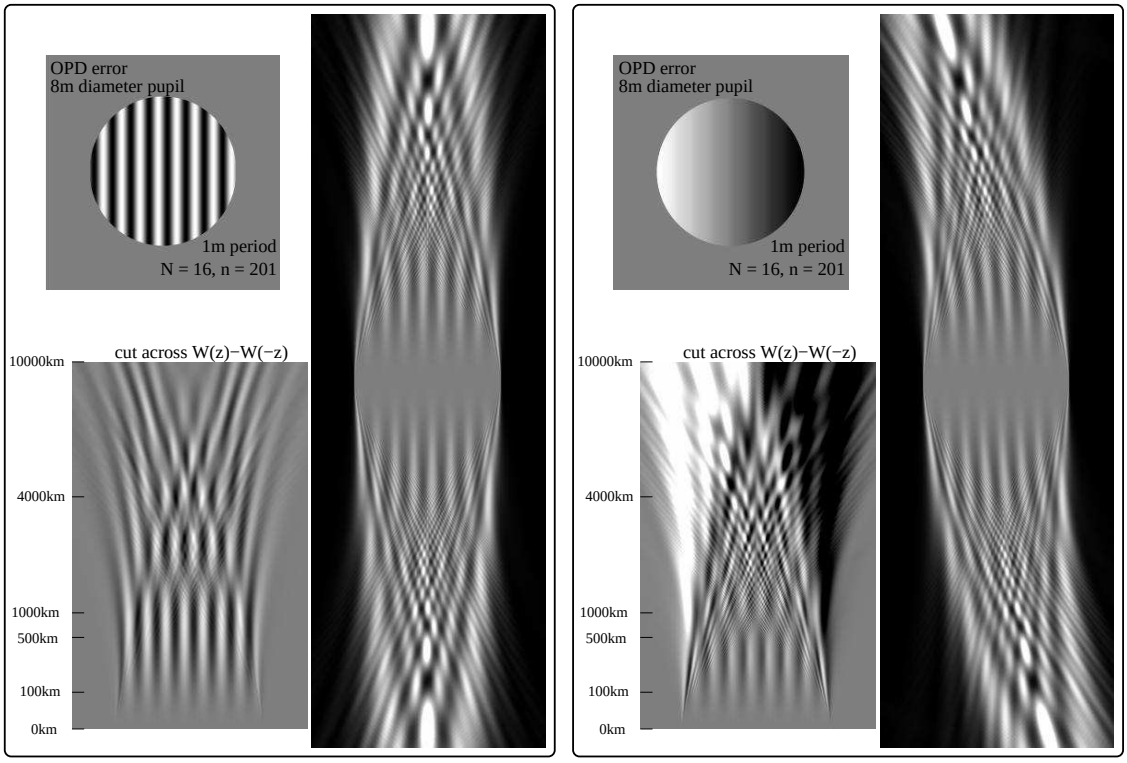

Figure 1. Non-linear effects in a curvature WFS. Each of the two panels shows wavefront phase (upper left), light intensity in a x/z plane, where x is the horizonatal coordinate in the pupil phase map and z is the defocus distance (right), and corresponding contrast in the x/defocus plane (lower left). Left panel: the linear relationship between wavefront curvature and intensity signal is only valid over a small range of defocus distance because of diffraction propagation effects. Right panel: a low order aberration (here tilt) distorts the pupil and further reduces the defocus range over which a linear signal can be extracted.

3. NON-LINEAR CURVATURE WAVEFRONT SENSOR

3.1. SIGNAL TO BE EXTRACTED

As shown in §2, conventional curvature WFS is strongly constrained by the requirement that wavefront sensor signals must be a linear function of the input wavefront aberrations:

- The linear constraint keeps the pupil defocus distance much smaller than it should be for optimal conversion of phase aberrations into intensity fluctuations. The dual stroke linear scheme described in §2.3 only slightly mitigates the negative effects of these constraints, but linearity is still enforced.
- A far more serious limitation is that linear reconstruction fully ignores the non-linear coupling between high and low order aberration in the defocused pupil images.

The performance to be gained by taking into account non-linear effects can best be understood for Tip-Tilt.

In linear curvature WFS, tip-tilt is measured as an overall displacement of the pupil in the defocused images: only the edges of the defocused pupil images are used to extract signal. For a small defocus distance, this displacement is proportional to the defocus distance dz: in conventional curvature WFS, dz is kept small for linearity to be maintained and the displacement is always a very small fraction of the pupil. Even if the defocus distance were infinitely large (as it would be in a curvature system designed only to measure tip-tilt), the tip-tilt sensitivity is at best equivalent to measuring the centroid of a λ/r_0-wide spot.

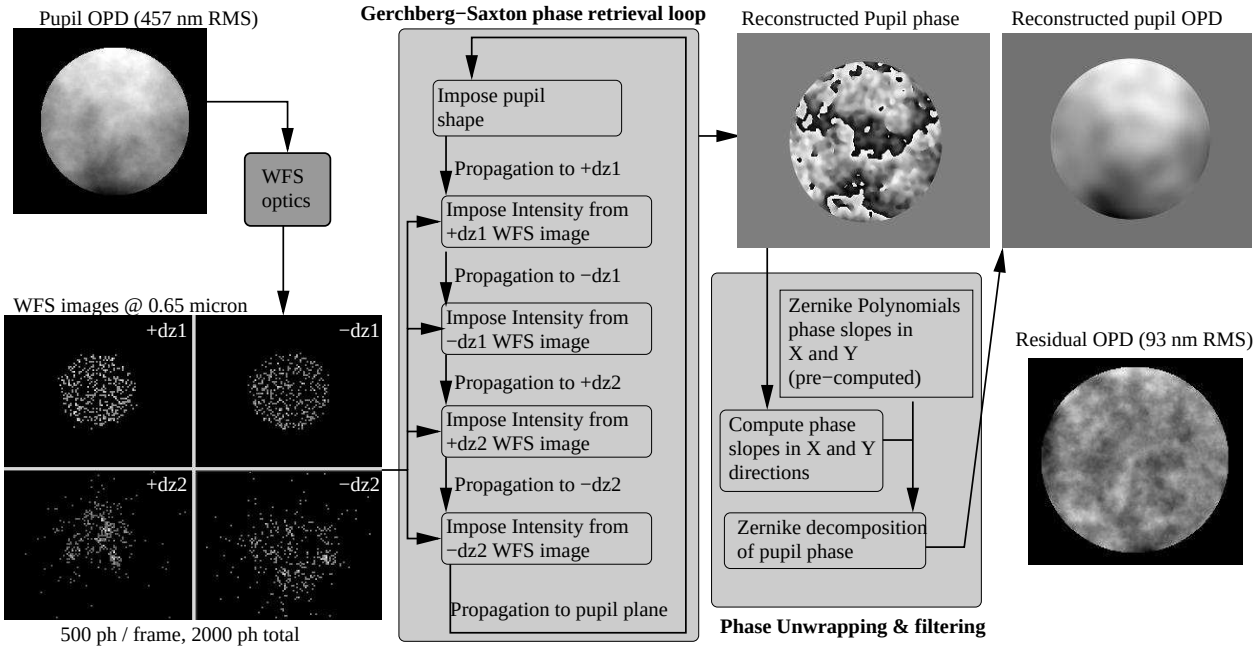

Figure 2. Wavefront reconstruction algorithm used in this work. See text for details.

If non-linear effects are to be taken into account for tip-tilt measurement, the WFS can be much more sensitive. First, larger defocus distances are allowed, which would improve the tip-tilt measurement sensitivity even if it were derived with the simple "pupil photocenter" diagnostic (which is linear). The real benefit is however found somewhere else: the defocused pupil images are "speckled" due to edge (pupil edge, central obstruction, spiders) diffraction effects and high order aberrations. These highly contrasted speckles, visible in Figure 3, are λ/D wide (which means they are physically smaller closer in to the pupil plane, and infinitely small - invisible - at the pupil plane). Provided that the defocused pupil image is acquired with proper spatial sampling, a tip-tilt can therefore be measured as the displacement of a "cloud" of λ/D-wide speckles. Of course, high order aberrations must be known to some degree to be able to recover this highly sensitive tip-tilt measurement. Similarly, low order aberrations need to be known to measure high order aberrations from the defocused pupil images.

A similar performance gain exists for other low spatial frequencies.

3.2. RECONSTRUCTION ALGORITHM

As shown in Figure 2, the reconstruction algorithm used in this work uses an iterative Gerchberg-Saxton type loop.[4,5] The defocused pupil images are used in this loop to constrain the amplitude (but not phase) in each of the four planes. Fresnel propagations between these planes are used to iteratively transform these amplitude constraints into a phase signal in the pupil plane. The result is a phase map in the 0 to 2π range: a linear phase unwrapping routine is then used to decompose the signal in a sum of wavefront modes (which can be Zernikes or other modes). The number of such modes should be chosen appropriately to match the quality of the data (photon / readout noise) and the number of elements of the deformable mirror.

Many iterations (typically 50) are needed to converge to a satisfactory result. It is however possible to considerably speed up the computation time by :

- "Fast-forwarding" the iterative loop. In most non-linear iterative loops, consecutive iterations produce a similar modification of the solution. It is therefore possible to multiply this modification by a constant larger than 1 before applying it to speed up the convergence. For the closed loop simulations performed in this paper, this constant was chosen to increase from 1 to ≈ 5 and then decease back to 1 during the full cycle of iterations.

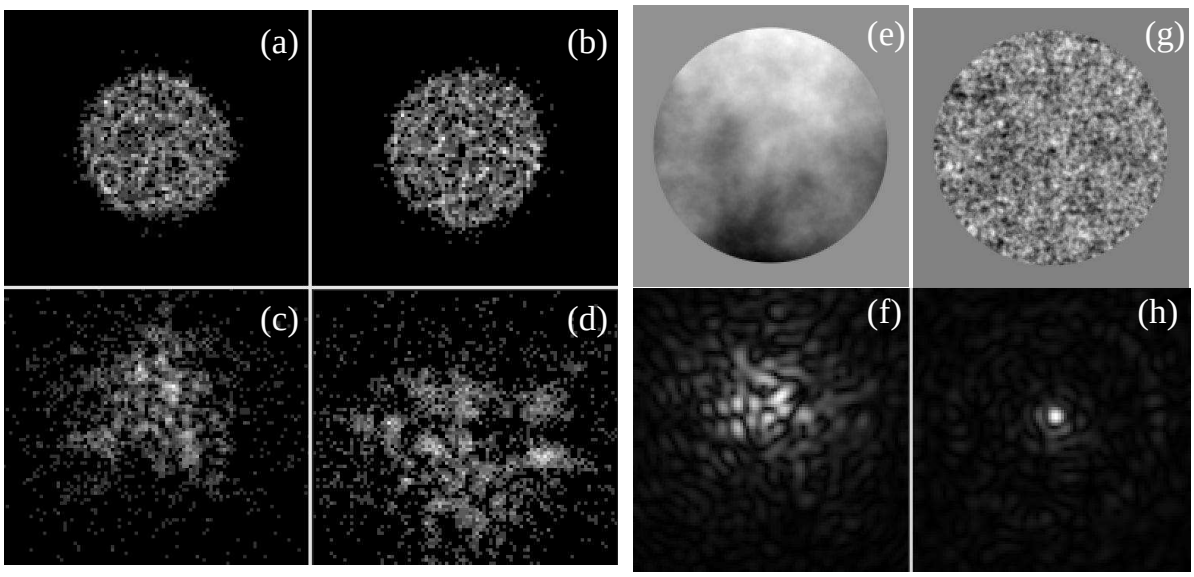

Figure 3. Example of a wavefront reconstruction performed on the defocused pupil images by the algorithm shown in Figure 2. Four noisy (photon noise) defocused pupil images (images (a), (b), (c) and (d)) are acquired to transform the pupil phase aberrations (e) into intensity signals. The input pupil phase is 609 nm RMS, yielding the PSF (f) before correction. After correction, the residual pupil phase aberration (g) is 34.4 nm RMS, allowing high Strehl ratio imaging (h). All images in this figure were obtained at 0.65 μm. The total number of photons available for wavefront sensing in 2e4.

- Start the loop with binned data. The algorithm shown in Figure 2 was first applied to binned data to quickly recover a low-accuracy wavefront estimate. This estimate is then used as the input of the higher accuracy non-binned loops.
- Apply a linear reconstructor first, and use the result as the starting point of the non-linear algorithm. This technique was not implemented for the simulations shown in this paper, but it should allow recovery of low order aberrations from the two images closest to the pupil plane.

Figure 3 shows how the non-linear wavefront reconstruction algorithm performs in monochromatic light for reconstruction of a wavefront with 609 nm error (RMS). With only 5000 photons in each of the four defocused pupil images, the non-linear reconstruction is able to recover the wavefront to within 34 nm, thus delivering a high Strehl image in the visible. As previously described, this performance is achieved by the ability to "track" λ/D wide features in the defocused images of the pupil, since these small features are highly sensitive to wavefront aberrations: low order aberrations would distort the pupil images and move the λ/D-wide speckles.

3.3. ROBUSTNESS

A significant advantage of performing the non-linear reconstruction from defocused pupil images (rather than images close to the focal plane) is that the defocused images are relatively achromatic. This is illustrated in Figure 4, where monochromatic and polychromatic ($d\lambda/\lambda = 0.5$) defocused pupil images are shown for a pupil with phase aberrations. Both sets of images are nearly identical, although small differences can be seen in the small structure of the highly defocused ($\pm$ 8000 km) images. Since the input images are very nearly achromatic, the non-linear curvature WFS should also be very insensitive to chromaticity. This is confirmed by simulations: with a $2\,10^8$ photons total, the non-linear reconstruction recovers the initial wavefront to within 9 nm in the monochromatic case, and 12 nm in the polychromatic case. Chromatic errors are therefore small, even though a monochromatic reconstructor was used on polychromatic data.

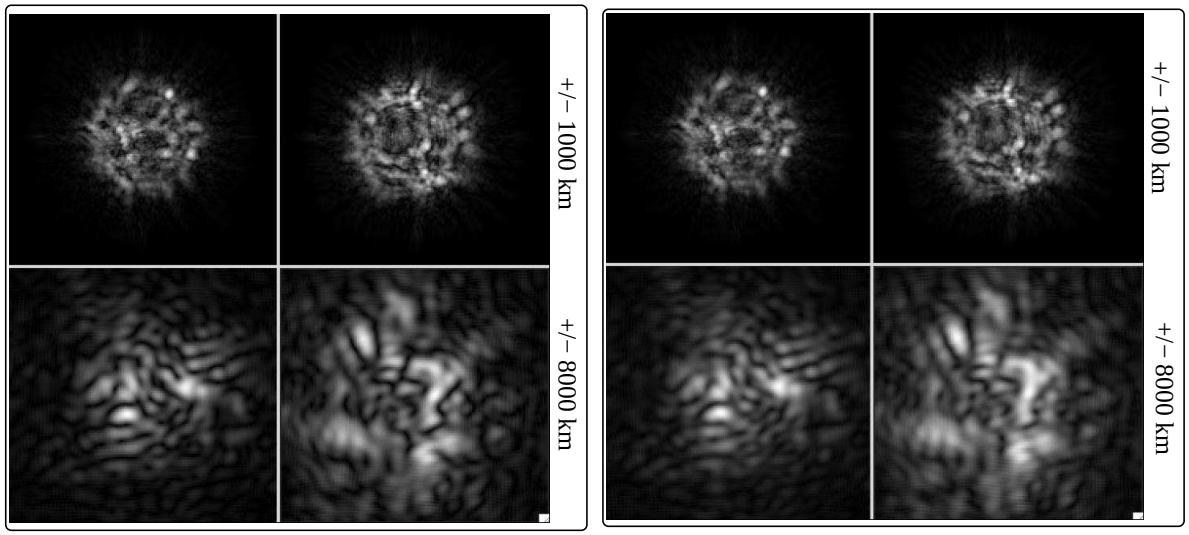

Figure 4. Monochromatic (left) and polychromatic (right) sets of defocused pupil images, showing that the non-linear curvature WFS scheme can work in polychromatic light with the same sensitivity. The polychromatic frames were simulated with a 50% wide spectral band.

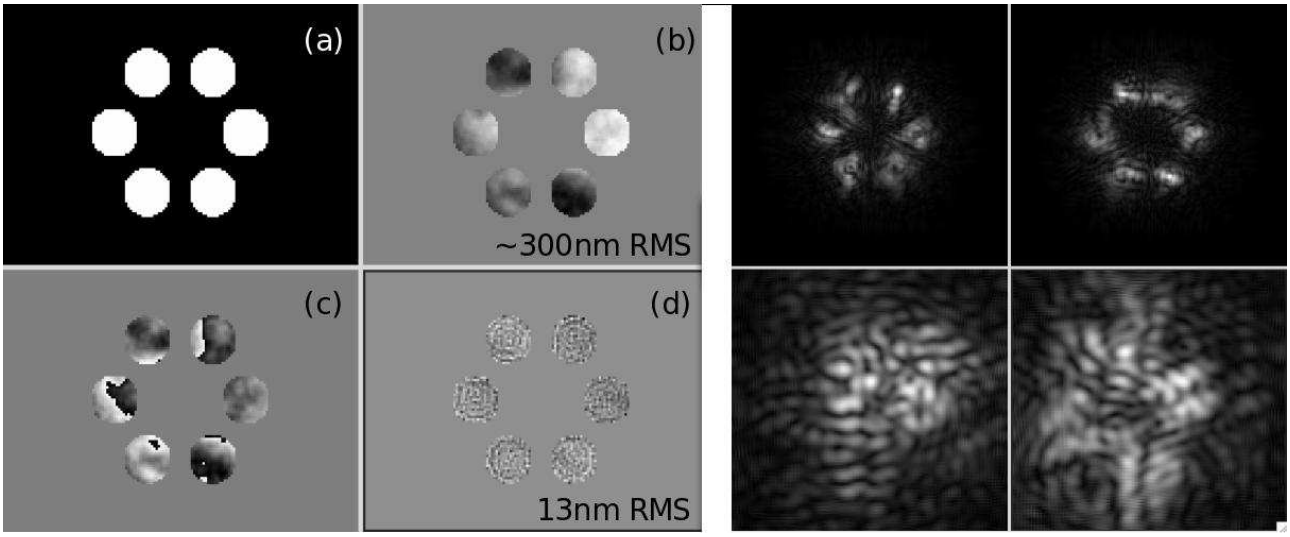

Figure 5. Demonstration of the non-linear curvature WFS's ability to recover wavefront errors on a sparse aperture. In this polychromatic simulation ($d\lambda/\lambda = 0.5$), both the wavefront inside each aperture and the differential piston between apertures are properly measured.

Non-linear curvature WFS also performs very well on sparse apertures, as demonstrated in Figure 5. Thanks to the large pupil defocus distance which the technique uses, light is efficiently mixed between the different segments of a sparse aperture, and the non-linear algorithm accurately recovers the differential piston between segments. The high sensitivity to these modes is equivalent to the high sensitivity to low order aberrations in a full pupil. With a SH WFS or a conventional curvature WFS, light would not be efficiently mixed between the segments.

4. PERFORMANCE

4.1. EXPECTED PERFORMANCE IN THE HIGH FLUX REGIME (EXTREME-AO)

In this section, the performance of non-linear curvature WFS is discussed in the high flux regime. Since the application considered here is Extreme-AO for high contrast coronagraphic imaging, the best performance metric is not Strehl (which would measure how much light is at the center of the PSF, and, in this regime, would always be very close to 1) but residual wavefront error at low spatial frequencies (these are the aberrations which scatter light where Extreme-AO systems try to build a "dark zone" in the PSF).

Table 2 lists, for several angular separations (corresponding to spatial frequencies in the pupil plane), the expected gain offered by moving from a SH WFS to a curvature WFS. The "flux gain" is the equivalent gain in guide star magnitude in the WFS, and the "contrast gain" is the corresponding PSF contrast factor which can be gained. For the "flux gain" to indeed offer the "contrast gain" listed, the AO loop speed must be increased to fully take advantage of the increased sensitivity. This may be a significant hardware and software challenge on bright stars, as loop speeds well above 10 kHz would be required.

Table 1. Performance Comparison Between SH WFS and non-linear curvature WFS

	Flux gain	Contrast gain
8m telescope, tip/tilt sensing	1600 (8.0 mag)	-
8m telescope, 2 l/d (41 mas)	180 (5.6 mag)	31.8 (3.8 mag)
8m telescope, 5 l/d (103 mas)	29 (3.6 mag)	9.4 (2.4 mag)
30m telescope, tip/tilt sensing	22500 (10.9 mag)	-
30m telescope, 2 l/d (11 mas)	2525 (8.5 mag)	185.4 (5.7 mag)
30m telescope, 5 l/d (28 mas)	404 (6.5 mag)	54.7 (4.3 mag)
30m telescope, 10 l/d (55 mas)	101 (5.0 mag)	21.7 (3.3 mag)

The gains listed in table 2 are very large, especially for the larger telescope size at small angular separations. On a 8m telescope, switching from a SH WFS to a non-linear curvature WFS is equivalent to making the guide star 5.6 mag brighter in the WFS for spatial frequencies corresponding to scattered light at 2 λ/d. This corresponds a 3.8 mag gain in contrast on the PSF. On a 30m telescope, also at 2 λ/d, the gains are respectively 8.5 mag in source brightness and 5.7 mag in PSF contrast. Gains are lower at higher angular separations, but are still very large. These results are especially encouraging for direct detection of exoplanets and imaging of protoplanetary disks, where the most critical requirement is to control extremely well low spatial frequencies.

4.2. PERFORMANCE IN THE INTERMEDIATE FLUX REGIME: CLOSED LOOP SIMULATIONS

In this section, the non-linear curvature WFS performance for intermediate flux sources (too faint for "true" Extreme-AO regime, but bright enough for the non-linear reconstruction to work properly) is evaluated by closed loop simulations. A fixed $3\,10^6$ ph/s flux, (corresponding to mag$\approx$13 with 20% efficiency over a $d\lambda/\lambda$=0.5 band) was adopted with a WFS working at 0.85 μm. The seeing was chosen at 0.6 arcsec at 0.55 μm, with a 10 m/s wind speed (single layer).

Closed loop images at 0.85 μm are shown in Figure 6 for several choices of WFS: SH WFSs with 4.5 to 30 subapertures across the pupil and non-linear curvature WFS. For SH WFSs, the DM was assumed to be perfect,

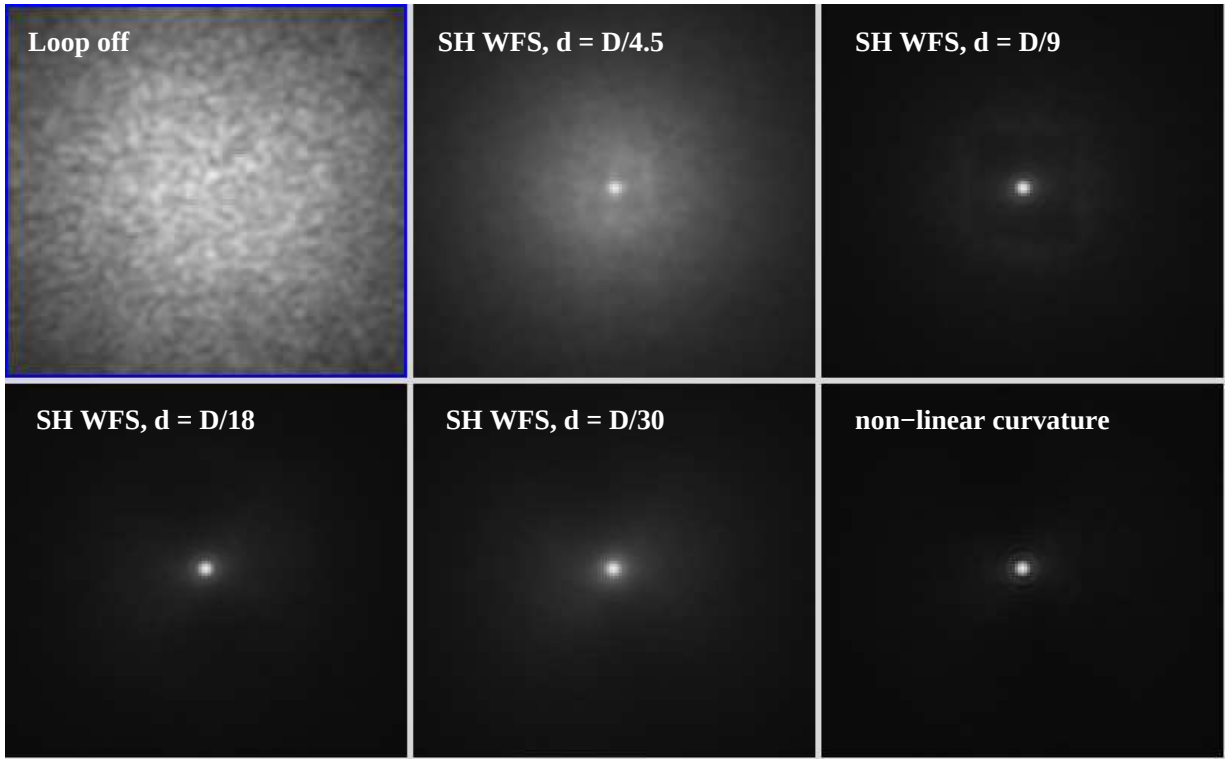

Figure 6. Comparison between closed-loop PSFs with several choices of WFS. All PSFs shown here are for a 20 sec integration at 0.85 μm. See text for details.

with a cutoff spatial frequency equal to the cutoff spatial frequency of the WFS. For the non linear curvature WFS, the DM was assumed to correct all modes up to 20 cycles per aperture. All simulations adopt a loop gain equal to 1 for all modes corrected (no modal control). The closed loop performance in each case, is also given in table 2.

Table 2. Performance Comparison Between SH WFS and non-linear curvature WFS

Wavefront Sensor	optimal loop frequency	Residual (RMS)
Non linear curvature	210 Hz	104 nm
SH, D/d = 4.5	160 Hz	315 nm
SH, D/d = 9	164 Hz	192 nm
SH, D/d = 18	166 Hz	182 nm
SH, D/d = 30	141 Hz	225 nm

The results obtained illustrate the trade-off between good sensitivity to low order aberrations and number of corrected modes for SH WFS. There is an optimal number of subapertures to minimize the residual wavefront error: with fewer subapertures, the fitting errors dominate, and with more subapertures, the error on the low order aberrations become too large (the PSF core is less contrasted). The non-linear curvature WFS is the only WFS to show both a sharp contrasted PSF core (good sensitivity to low order aberrations) and control of a large number of modes (low fitting errors).

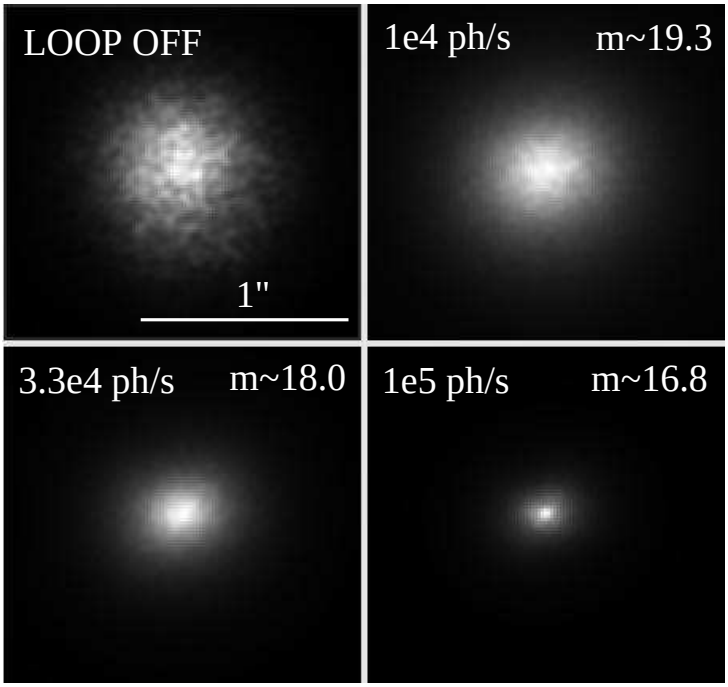

Figure 7. Uncorrected (upper left) and closed loop simulated 1.6 μm images with a non-linear curvature WFS operating at 0.85 μm. Approximate magnitude values are given assuming a 20% efficiency and a $d\lambda/\lambda = 0.5$ spectral band.

4.3. PERFORMANCE IN THE LOW FLUX REGIME

The high sensitivity of the non-linear curvature WFS relies on the ability to "track" λ/D-wide speckles in the defocused pupil images. As the number of available photons decreases, since these small speckles have a finite lifetime, there is not enough light to resolve these fine structures in the defocused images. The WFS performance is then expected to rapidly drop. Closed-loop simulations have been performed to investigate the behaviour of the non-linear curvature WFS in the low flux regime. It was indeed found that the performance rapidly falls at around 200000 ph/s on a 8-m telescope with 0.6 arcsec seeing and a 10 m/s wind speed. Interestingly, this transition occurs at lower flux levels if the wavefront sensor wavelength is increased: it is possible to maintain coherence in the WFS by increasing the wavelength. For sensing at 0.7 μm, the transition occurs at 500000 ph/s ($m \approx 15$), while for sensing at 1 μm, it occurs at 200000 ph/s ($m \approx 16$).

In the low flux regime (source fainter than the transition described above), the non-linear curvature WFS algorithm is still stable. Performance is then close to a linear WFS and the closed-loop PSF becomes closer to the uncorrected PSF as flux is reduced, as shown in Figure 7.

5. CONCLUSION

The non-linear curvature WFS technique described in this paper offers very high sensitivity while maintaining a good enough dynamical range to also be advantageous for fainter stars. Its performance in the low aberration regime is similar to a pyramid WFS operating in the "fixed pyramid" mode (no modulation), it appears to be more tolerant to large wavefront errors, and can therefore operate at optical wavelength where the AO system may not be able to deliver a sharp high Strehl PSF.

This technique appears especially well suited for Extreme-AO applications, where high sensitivity to low order aberrations is essential in order to reduce scattering at small angular separation from a bright star.

REFERENCES

[1] Guyon, O. 2005, ApJ, 629, 592
[2] Roddier, F., Northcott, M., Graves, J.E. 1991, PASP, 103, 131
[3] Guyon, O., Blain, C., Takami, H., Hayano, Y., Hattori, M., Watanane, M. 2008, PASP, in press
[4] Gerchberg, R.W., Saxton, W.O. 1972, Optik, 35, 237
[5] Fineup, J.R. 1982, Appl. Opt. 21, 2758